Ethanol and Hydrogen Gas-Sensing Properties of $CuO–CuFe_2O_4$ Nanostructured Thin Films

Saptarshi De, Narayanan Venkataramani, *Senior Member, IEEE*, Shiva Prasad, Rajiv Onkar Dusane, Lionel Presmanes, Yohann Thimont, Philippe Tailhades, Valérie Baco-Carles, Corine Bonningue, Sumangala Thondiyanoor Pisharam, and Antoine Barnabé

***Abstract*— Nanocrystalline $CuO–CuFe_2O_4$ composite thin films were developed from $CuFeO_2$ ceramic target using a radio-frequency sputtering method followed by a thermal oxidation process. This fabrication process helps to develop porous sensing layers which are highly desirable for solid-state resistive gas sensors. Their sensing properties toward ethanol and hydrogen gas in dry air were examined at the operating temperatures ranging from 250 °C to 500 °C. The electrical transients during adsorption and desorption of the test gases were fitted with the Langmuir single site gas adsorption model. A composite thin film with a total thickness of 25 nm showed highest response (79%) toward hydrogen (500 ppm) at the operating temperature of 400 °C. The shortest response time (τ_{res}) was found to be ∼60 and ∼90 s for hydrogen and ethanol, respectively. The dependence of the response of the sensor on gas concentration (10–500 ppm) was also studied.**

***Index Terms*— Ethanol, gas sensor, hydrogen, nanocrystalline $CuO–CuFe_2O_4$, thin film.**

I. Introduction

METAL oxide semiconductors (MOS), such as pure CuO phase or CuO coupled with other MOS in a composite material, have been used as sensor materials for many years for the detection of reducing gases such as hydrogen [1], [2], ethanol [3]–[7], CO [8], [9], and H_2S [10]–[12]. Recently, various nano structures of CuO like one-dimensional (1D) nano wire and thin films have caught attention due to high surface to volume ratio which is expected to enhance the performance of the devices based on semiconductor nano structures [13]. Porous CuO nano wires [14], CuO/ZnO hetero contact sensors [15] and Zn doped CuO nano wires [16] were reported for improving H_2 detection. In addition with all the gases listed above, CuO can also be interesting for CO_2 detection [17]. On the other hand, copper based spinel oxides such as copper ferrite ($CuFe_2O_4$) having n-type semiconductor properties was also reported to show response toward H_2 [18], LPG [19] and ethanol [20]. In our previous work, maximum response (ΔR/R) of 86% was obtained by $CuFe_2O_4$ nano powder toward 500 ppm of ethanol [21], and this pure copper ferrite also showed a good response of 10% toward CO_2 [22].

Semiconductor nano composites with p–n junction were reported as a subject of interest for gas sensing regarding operating temperature (O.T.) and response. In particular, many authors have studied the combination of p-type CuO with various n-type oxides for CO_2 detection [23]–[26]. In the recent past, $CuO/CuFe_2O_4$ composite thin films [27] and powders [22] having spinel phase were also reported as CO_2 gas sensing material.

In this work, nanocrystalline $CuO–CuFe_2O_4$ semiconductor thin films were developed from $CuFeO_2$ ceramic target using a radio-frequency (RF) sputtering method followed by a thermal oxidation process. This fabrication process may help to develop porous sensing layers which are highly desirable for solid state resistive gas sensors. These films were used as the sensitive material for reducing gases like hydrogen and ethanol. The effect of the operating temperature on the response, response time and recovery time of the active layer were studied to evaluate the merit of performance of the material. The effect of gas flow rate on the response time and recovery time of the active layer were also studied. To demonstrate its potential sensing application, the variation of response with different gas concentration has been shown. Here, the minimum operating temperature was chosen as 250 °C to avoid the effect of moisture on sensor samples during practical gas sensing application. We also tried to generate the values of activation energy for the gas (H_2) adsorption and intrinsic reaction on CuO thin film surface using Langmuir gas adsorption model, which may be useful in future to compare with other sensing material and gases for analysing the gas sensing properties.

II. Preparation of the Gas Sensitive Layers

$Cu–Cu_xFe_{3-x}O_4$ thin films were first deposited on fused silica substrate at room temperature with Alcatel A450 RF sputtering unit using a pure delafossite ($CuFeO_2$) ceramic target. The details of the deposition procedure were described

Manuscript received April 1, 2018; revised June 11, 2018; accepted June 17, 2018. Date of publication June 20, 2018; date of current version August 10, 2018. This work was supported in part by the MonaSens Project DST under Grant 14IFCPAR001and in part by ANR under Grant 13-IS08-0002-01. The associate editor coordinating the review of this paper and approving it for publication was Dr. Camilla Baratto. *(Corresponding author: Narayanan Venkataramani.)*

S. De, N. Venkataramani, and R. O. Dusane are with the Department of Metallurgical Engineering and Materials Science, Indian Institute of Technology Bombay, Mumbai 400076, India (e-mail: sapjaki@gmail.com; ramani@iitb.ac.in).

S. Prasad is with the Department of Physics, Indian Institute of Technology Bombay, Mumbai 400076, India, and also with the Institute of Infrastructure Technology Research and Management, Ahmedabad 380 026, India.

L. Presmanes, Y. Thimont, P. Tailhades, V. Baco-Carles, C. Bonningue, S. T. Pisharam, and A. Barnabé are with Centre Interuniversitaire de Recherche et d'Ingénierie des Matériaux, Université de Toulouse, CNRS, INPT, UPS, F-31062 Toulouse, France (e-mail: barnabe@chimie.ups-tlse.fr).

Digital Object Identifier 10.1109/JSEN.2018.2849330

TABLE I

DEPOSITION PARAMETERS FOR THE SPUTTERING

Target	$CuFeO_2$
Magnetron	No
RF power (W)	200
Argon pressures (Pa)	0.5
Target to substrate distance (cm)	5
Substrate	Fused silica
Deposition rates (nm/min)	6.8

by Barnabé *et al.* [28]. Process parameters for the room temperature deposited samples are given in Table I. Two films having thicknesses 25 nm and 300 nm were deposited by varying the deposition time. Thickness of the deposited films was measured using a Dektak 3030ST profilometer and cross-sectional scanning electron microscopy (SEM) using JEOL JSM 6700F field emission SEM. Our previous studies (i.e. grazing incidence X-ray diffraction (GI-XRD), Raman spectroscopy and electron probe micro analysis (EPMA)) on the same samples have already revealed that the as-deposited films consisted of copper nano particles which were embedded in an oxide matrix which was made of cuprous oxide and mixed valence defect ferrite (Cu_2O, $Cu_xFe_{3-x}O_4$) [28], [29] (Equation 1a). In order to obtain the stable $CuO/CuFe_2O_4$ nano composite, the as-deposited films were ex-situ annealed at 550 °C in air for 12 h (Equation 1b). The tenorite phase CuO then originated from the oxidation of the metallic copper in association with that of Cu_2O. One can note that the reaction scheme could be more complex if we consider the formation of $CuFeO_2$ intermediate phase [29]. The annealing treatment of the as-deposited samples starting from delafossite target can be represented by the following simplified reaction scheme:

1) reduction during deposition step

$$\underset{\text{(Target)}}{CuFeO_2} \rightarrow \underset{\text{(as-deposited film)}}{x\ Cu + (1-x)/2\ Cu_2O + (9-x)/24\ Fe_{24/(9-x)}O_4} + x/3\ O_2 \quad (1a)$$

2) oxidation during post deposition annealing

$$\underset{\text{(as-deposited film)}}{x\ Cu + (1-x)/2\ Cu_2O + (9-x)/24\ Fe_{24/(9-x)}O_4} + (4x+3)/12\ O_2 \rightarrow \underset{\text{(annealed film)}}{x/2\ CuO + x/2\ CuFe_2O_4} \quad (1b)$$

The SEM image in figure 1 shows that, as a result of annealing, the parent films were self-organized in a two layered stack with top to bottom layer thickness ratio of 1:2. These films were characterized by GI-XRD technique and Glow-discharge optical emission spectroscopy (GD-OES) profile [27] and X-ray photo electron spectroscopy (XPS) [29] which confirmed that the top layer was tenorite CuO and that of the bottom layer was spinel $CuFe_2O_4$.

Interestingly, a 30% increase in the total thickness of the as-deposited thin film was observed after annealing which was possibly due to the porosity developed during post-deposition annealing [29]. This porosity in the two layered stack might be caused by the metallic copper diffusion during the oxidation process of the as-deposited samples. For thin film semiconductor metal oxide based gas sensors, the porosity of the sensing layer is an important parameter [30] as the gas diffusion through the porosity can cause changes in electrical properties of the films, making the gas detection easier.

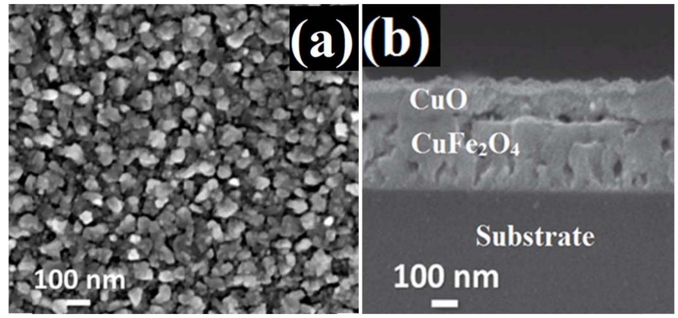

Fig. 1. FE-SEM micrographs (a) plain view and (b) cross section view of the sample annealed at 550 °C for 12 hours in air.

III. GAS SENSING MEASUREMENTS

Gas sensing experiments were carried out in a closed chamber with controlled operating temperature from 250 °C to 500 °C using a PID controller. The ambient gas environment was controlled by a continuous flow of the calibrated test gases or air using mass flow controller. For the hydrogen sensing, two gas cylinders were used- one with just zero air (moisture $< 0.01\%$) and another with same zero air containing 500 ppm of hydrogen. The sensor samples were stabilized at each operating temperatures for at least 12 hours in zero air, prior to the gas sensing experiment. Resistance-transients of the sensing layer were measured in two probes mode using Keithley 2635B source meter. Similarly, for the ethanol sensing experiments, two gas cylinders were used, one with zero air and another with the same zero air containing 500 ppm of ethanol. The response (R_s) of the sensor samples is defined as the relative difference of the film resistance between air and test gas atmosphere (R_{gas}-R_{air})/ $R_{air} \times 100\%$, where R_{gas} and R_{air} are saturated resistance of the sensor in test gas atmosphere and in air respectively. The concentration of the test gases ($C_{gas\ in\ chamber}$) in the gas chamber was varied by diluting with zero air, and it can be calculated using the following relation:

$$C_{gas\ in\ chamber} = [C_{test\ gas} x (dV_{test}/dt)]/[(dV_{test}/dt) + (dV_{zero\ air}/dt)] \quad (2)$$

Where $C_{test\ gas}$ is the concentration of the test gas in gas cylinder and dV_{test}/dt is the volumetric flow rate of test gas, similarly $dV_{zeroair}/dt$ is the volumetric flow rate of zero air.

IV. RESULTS AND DISCUSSION

Figure 2 shows the resistance-transients during the insertion of hydrogen (500 ppm) and recovery in air of the 25 nm thin film sensor at the operating temperature of 400 °C with 100 cc/min gas-flow rate. The sensing material showed good repeatability as the initial baseline was regained upon exposure to dry air. The increase in the electrical resistance of the

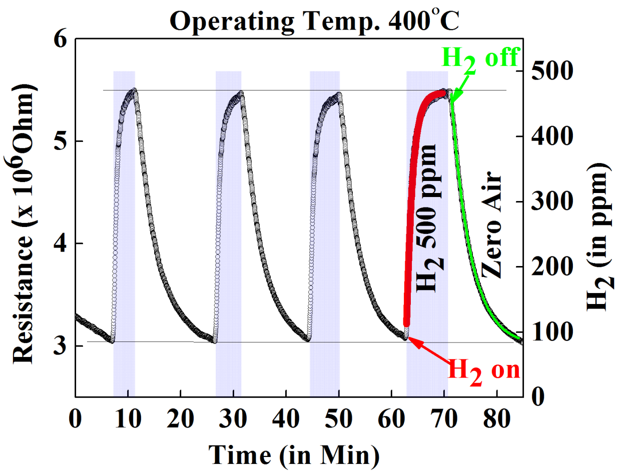

Fig. 2. Resistance-transients (response and recovery) of the 25 nm thin film sensor at the operating temperature of 400 °C with 100 cc/min flow rate, fittings are shown in coloured lines.

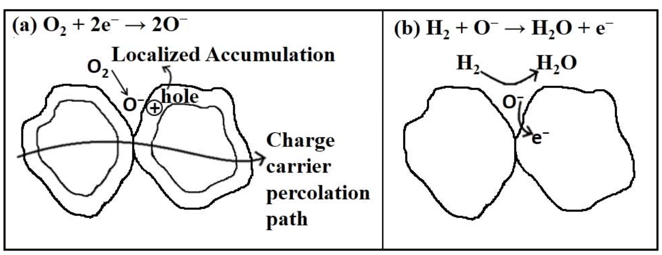

Fig. 3. Schematic of the proposed sensing mechanism- (a) during stabilization of the sensor material (oxygen adsorption); (b) during sensing of the test gas (e.g. hydrogen).

sensors upon exposure to a reducing gas such as H_2 indicates that the obtained films have p-type semiconducting behaviour. It could be possible that only CuO is involved in sensing as it is the top layer.

The following reaction mechanism for the sensing of reducing gas by a p-type semiconductor can be summarized from several research reports [3]. In a first step, at the operating temperature, oxygen is physisorbed on the sensor surface followed by electron transfer from the p-type semiconducting oxide CuO to the adsorbed oxygen, thus forming chemical bond between the adsorbed oxygen and the semiconducting oxide. Thus, the electrical resistance of the p-type semiconductors reduces during stabilization of the sensor material [see figure (3.a)].

These reactions are described in equations (3) and (4) respectively

$$\frac{1}{2}O_2 + [\text{sensor}_{\text{surface}}] \leftrightarrow O_{\text{ad-surface}}\ (\text{physisorption}) \quad (3)$$

$$O_{\text{ad-surface}} + e^- \leftrightarrow O^-_{\text{ad}}\ (\text{chemisorption}) \quad (4)$$

When the sensor is exposed to reducing gas ambient, the reducing gas is physically adsorbed on the active layer surface and reacts with the adsorbed oxygen according to the reaction (5) & (6) and the product (RO) goes out [eq. 7] [see figure (3.b)]. Thus, the resistance of the p-type sensor increases.

$$R + [\text{sensor}] \leftrightarrow R_{\text{ad}}(\text{physisorption}) \quad (5)$$

$$R_{\text{ad}} + O^-_{\text{ad}} \leftrightarrow RO_{\text{ad}} + e^- \quad (6)$$

$$RO_{\text{ad}} \leftrightarrow RO_{\text{gas}}\uparrow + [\text{sensor}_{\text{surface}}] \quad (7)$$

Out of these reactions, the physisorption of oxygen as well as that of the reducing gas [Eq. (3) and (5)] are fast. On the other hand the reaction between the adsorbed gas and oxygen [Eq. (6)] is a slow process and therefore, the last one is the rate determining step for the response kinetics. This is easily corroborated from the reported data on surface reaction of adsorbed oxygen [31] and hydrogen [32]. According to Ahn *et al.* [31], the ratio of surface reaction rate constant to adsorption rate constant at adsorption equilibrium for oxidation of sulphur dioxide is 0.5, and Arrua *et al.* [32] reported the same ratio for hydrogenation using Pd/Al_2O_3 catalyst in the range of 0.26-0.29. Assuming Langmuir single site gas adsorption model for the thin film sensors [33], the response and the recovery transients were fitted well with the following two equations (eq. 8, 9) respectively (shown in coloured lines in fig. 2). The values of coefficient of determination (R^2) in this fitting for all response or recovery curves were in between 0.985-0.999.

$$R(t)_{\text{response}} = R_{\text{air}} + R_1[1 - \exp(-t/\tau_{\text{res}})] \quad (8)$$

$$R(t)_{\text{recovery}} = R_{\text{air}} + R_1[\exp(-t/\tau_{\text{rec}})] \quad (9)$$

Where τ_{res} and τ_{rec} are the 'response time' and 'recovery time' respectively. And R_1 is a proportionality constant of the exponential term whose value is equal to the difference of the film resistance between air and test gas atmosphere (R_{gas}-R_{air}).

The variation of response and recovery time with gas flow rate was observed and tabulated in Table II. Decrease in response and recovery time with gas flow rate indicates a mass transfer controlled reaction kinetics on this thin film surface. Therefore, the flow rate was kept fixed at 100 cc/min for the rest of the experiments performed.

TABLE II

VARIATION IN RESPONSE TIME AND RECOVERY TIME WITH GAS-FLOW RATE AT A FIXED OPERATING TEMPERATURE (500 °C); 25 nm COMPOSITE THIN FILM

Gas flow rate (in cc/min)	τ_{res} (in s)	τ_{rec} (in s)
20	137	221
50	82	190
100	63	131

Hydrogen sensing by a 25 nm thin film sensor was carried out at different operating temperatures and the variation of response time and recovery time are given in the table III. Response time seemed to be saturated above the operating temperature of 350 °C and the saturated value was found to be around 60 seconds. At the high operating temperatures, the reaction rate of eq. (6) became faster and the reaction might be limited by the test conditions, i.e., gas flow in the gas chamber. Recovery time decreased monotonically with the operating temperature until 500 °C.

TABLE III

VARIATION IN RESPONSE TIME AND RECOVERY TIME OF 25 nm THIN FILM SENSOR WITH THE OPERATING TEMPERATURE (TEST GAS: 500 ppm OF H_2 WITH 100 cc/min FLOW RATE)

Operating Temperature (in °C)	τ_{res} (in s) (error)	τ_{rec} (in s) (error)
250	276 (±11)	667 (±27)
300	116 (±5)	416 (±17)
350	58 (±3)	249 (±10)
400	58 (±3)	221(±9)
450	56 (±3)	186 (±8)
500	63 (±3)	131(±6)

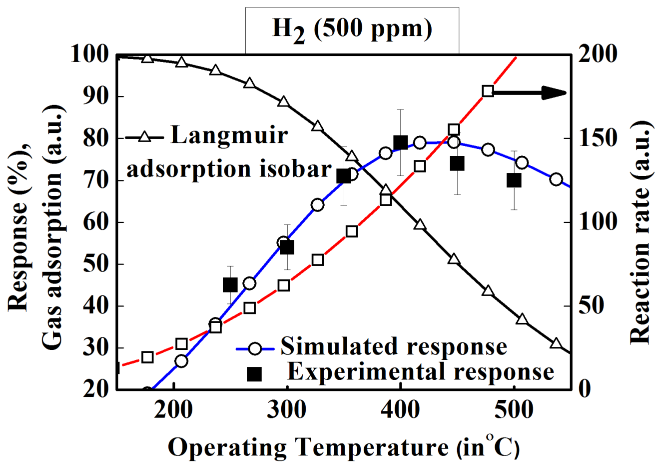

Fig. 4. Experimental and simulated response vs. operating temperature of 25 nm composite thin film (test gas: 500 ppm of H_2 with 100 cc/min flow rate).

The bell shaped response curve with the operating temperature as shown in the figure 4 is a result of the competitive behaviour of eqs. (5) and (6). Similar bell shaped response curve had been reported by Ahlers *et al.* [34] and Biswas and Pramanik [35]. According to them, response varies with operating temperature on the basis of two energy systems. E_{ads} is dependent on the strength of the test gas binding onto the sensing material surface. On the other hand, E_a is defined as the energy barrier required to be overcome by the adsorbed gas molecules for diffusion along the surface, resulting in catalysis induced surface combustion process. Initially, under clean air conditions, active sites on the surface of a sensor material had been covered by adsorbed oxygen. Then, relative occupancy of the test gas on the pre-adsorbed oxygen depends on partial pressure and operating temperature of the test gas. In the figure 4, simulated curves of Langmuir relative surface coverage (L), reaction rate (K) and the modeled response (R_m) are shown. Here,

$$L = \frac{Pgas}{Pgas + Po} \tag{10}$$

where P_{gas} is partial pressure of test gas (H_2) at sensing layer and $P_o = \frac{k_B T}{Vo} \exp\left(\frac{-Eads}{k_B T}\right)$, where v_o is the quantum volume of the test gas species, given by $v_o = \left(\frac{2\pi\hbar^2}{M_{gas} M_o k_B T}\right)^{1.5}$, where M_{gas} is the relative atomic mass of the test gas (i.e. 2 for H_2); M_o is the atomic mass unit (1.67×10^{-27} kg); $\hbar$ is the reduced plank constant and k_B, T are Boltzmann constant and absolute temperature respectively. The reaction rate of adsorbed test gas with chemisorbed oxygen ion is

$$K = A \exp\left(\frac{-Ea}{k_B T}\right) \tag{11}$$

where A is a proportionality constant. The modeled response was obtained from the combination of Langmuir relative surface coverage and the reaction rate [34], and it could be given by

$$R_m = \frac{Pgas}{Pgas + \frac{k_B T}{Vo} \exp\left(\frac{-Eads}{k_B T}\right)} A \exp\left(\frac{-Ea}{k_B T}\right) \tag{12}$$

In the case of tin dioxide (SnO_2) thin film sensors, the values of E_{ads} varied from 130 to 145 kJ/mol (1.3-1.45 eV) and E_a varied from 53 to 57 kJ/mol (0.53-0.57 eV) for different ethane concentrations [34]. Here, the values E_{ads} and E_a were obtained (by the fitting of experimental values with eq. 12) as 43 kJ/mol (0.45 eV) and 21 kJ/mol (0.22 eV) respectively. This sensor sample showed maximum response of 79% at the operating temperature of 400 °C toward 500 ppm of H_2. A similar response of 70% was reported for H_2 but at a higher concentration (2500 ppm) with thicker copper oxide–copper ferrite sensor system [36]. Hoa *et al.* [2] reported 40% response toward 10,000 ppm of H_2 at an operating temperature of 250 °C for CuO thin film, whereas at the same operating temperature, this $CuO/CuFe_2O_4$ thin film exhibits 45% response only at 500 ppm of H_2.

TABLE IV

CHANGE IN RESPONSE TIME AND RECOVERY TIME OF 25 nm THIN FILM SENSING MATERIAL WITH THE OPERATING TEMPERATURE (TEST GAS: 500 ppm OF ETHANOL WITH 100 cc/min FLOW RATE)

Operating Temperature (in °C)	τ_{res} (in s) (error)	τ_{rec} (in s) (error)
250	432 (±17)	740 (±30)
300	223 (±9)	440 (±18)
350	150 (±6)	370 (±15)
400	121 (±5)	390 (±16)
450	90 (±4)	450 (±18)
500	90 (±4)	480 (±19)

Similarly, ethanol sensing of the 25 nm thin film sensor was carried out at different operating temperatures and the variation of response time and recovery time are given in the table IV. Response time seemed to be saturated above the operating temperature of 450 °C and the value of that was found to be around 90 seconds. It was observed that the recovery time decreased to the range of 350 to 400 °C and after that it had increased. This increase at 500 °C is not well understood at present. Figure 5 shows the variation of response with operating temperature. In case of ethanol, the maximum response of this thin film sensor might be observed above 500 °C. As per literature, the best operating temperature to get maximum response for ethanol was reported to be higher than that of hydrogen [37]. The operating temperature was confined below 500 °C due to the (a) stability of the phase and microstructure in sensing layers and (b) instrumental limitation. Hence we may not be able to capture a similar behaviour as found in H_2.

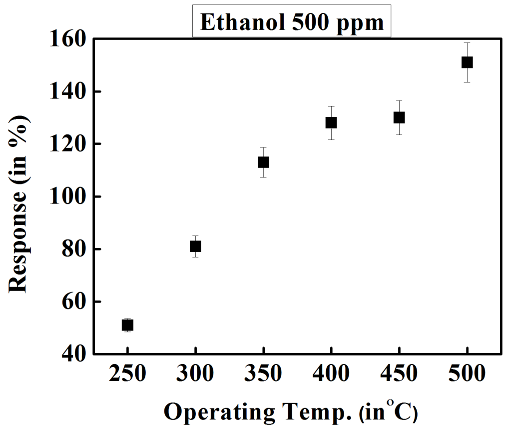

Fig. 5. Response vs. operating temperature of 25 nm thin film sensing material (test gas: 500 ppm of ethanol with 100 cc/min flow rate).

TABLE V
RESPONSE TIME, RECOVERY TIME AND RESPONSE VS. FILM-THICKNESS

Thickness of films (nm)	Test gas (500 ppm)	Operating Temperature (°C)	τ_{res} (s)	τ_{rec} (s)	R_s (%)
25	Ethanol	450	90	450	130
300	Ethanol	450	204	800	114
25	H_2	400	58	221	79
300	H_2	400	230	790	68

Here, due to lack of the bell shape in the response curve, it could not be fitted with the chosen model (eq.12).

The gas sensing experiment was carried out with 300 nm thick film and the results are tabulated in table V. Thicker $CuO–CuFe_2O_4$ thin film showed p-type response toward reducing gases, i.e., hydrogen and ethanol. So, the test gases were mostly interacting (adsorption/desorption) with the copper oxide layer located on the top of film.

Depending on the operating temperature, oxygen molecules adsorbed on semiconductor surface are in various ionic states, i.e. O_2^-, O^- or O^{2-} [38]. So, adsorbed hydrogen (H_{2ads}) may react with adsorbed oxygen (O_{ads}^{ion}) as in the following equations.

$$2H_{2\ ads} + O_2{}^-{}_{ads} \rightarrow 2H_2O + e^- \quad (13)$$

or,

$$H_{2\ ads} + O_{ads}^- \rightarrow H_2O + e^- \quad (14)$$

or,

$$H_{2\ ads} + O_{ads}^{2-} \rightarrow H_2O + 2e^- \quad (15)$$

Similarly, carbon dioxide and water are the final decomposition products of ethanol combustion in air. Acetaldehyde or acetic acid may also form as intermediate products during the oxidization of ethanol. Hence depending on the types of adsorbed oxygen and by-products of ethanol, various charge balance equations of ethanol decomposition are possible and given below.

$$\left.\begin{array}{l} 2CH_3CH_2OH_{ads} + O_2{}^-{}_{ads} \rightarrow 2CH_3CHO + 2H_2O + e^- \\ CH_3CH_2OH_{ads} + O_{ads}^- \rightarrow CH_3CHO + H_2O + e^- \\ CH_3CH_2OH_{ads} + O_{ads}^{2-} \rightarrow CH_3CHO + H_2O + 2e^- \\ CH_3CH_2OH_{ads} + O_2{}^-{}_{ads} \rightarrow CH_3COOH + H_2O + 1e^- \\ CH_3CH_2OH_{ads} + 2O_{ads}^- \rightarrow CH_3COOH + H_2O + 2e^- \\ CH_3CH_2OH_{ads} + 2O_{ads}^{2-} \rightarrow CH_3COOH + H_2O + 4e^- \\ CH_3CH_2OH_{ads} + 3O_2{}^-{}_{ads} \rightarrow 2CO_2 + 3H_2O + 3e^- \\ CH_3CH_2OH_{ads} + 6O_{ads}^- \rightarrow 2CO_2 + 3H_2O + 6e^- \\ CH_3CH_2OH_{ads} + 6O_{ads}^{2-} \rightarrow 2CO_2 + 3H_2O + 12e^- \end{array}\right\} \quad (16)$$

From equations (13), (14) and (15), for all metal oxide sensors a general rate equation of electron density can be written as

$$\frac{dn}{dt} = K_{gas}(T)[O_{ads}^{ion}]^a[R]^b \quad (17)$$

where, n is the electron density or electron concentration in the charge accumulation layer under the test gas (e.g. H_2) atmosphere, b is a charge parameter which might have value in the range of 0.5 to 2 for hydrogen and 0.08 to 2 for ethanol respectively. Similarly, a is a charge parameter which might have value in the range of 0.5 to 1 for oxygen ions. $K_{gas}(T)$ is the reaction rate constant or reaction rate coefficient described as

$$K_{gas}(T) = A\ \exp(-E_a/k_BT) \quad (18)$$

where E_a is the activation energy of reaction, k_B is the Boltzmann constant, T is absolute temperature and A is proportionality constant. Integrating Eq. (17) leads to the solution as

$$n = K_{gas}(T)[O_{ads}^{ion}]^a[R]^bt + n_o \quad (19)$$

where n_o is the saturated electron concentration of sensor at an operating temperature in the air atmosphere. In the saturated ethanol, i.e., at equilibrium under ethanol and air atmosphere, carrier concentration n and n_o could be considered as a constant with time.

$$n = K_{gas}(T)[O_{ads}^{ion}]^a[R]^b\tau + n_o \quad (20)$$

Where τ is a time constant. At a constant operating temperature the resistivity of a semiconductor is defined as $\rho = \alpha$ / n. Where α is a proportionality constant with '+' sign for n-type and '−' sign for p-type semiconductor, and can be substituted in equation (20) as

$$\frac{1}{Rg} = (K_{gas}(T)[O_{ads}^{ion}]^a[R]^b\tau)/\alpha + \frac{1}{Ra} \quad (21)$$

Assuming the concentration of adsorbed test gas ($[R]^b$) on the sensor surface is linearly proportional to the gas concentration in gas chamber (C_g^b), at constant operating temperature the sensor response relation can be obtained in a compact form

$$R_s = MC_g^b \quad (22)$$

where R_s is response of the sensor and it could be defined as $(R_{gas}\text{-}R_{air})/R_{air}$ and M is $(K_{gas}(T)[O_{ads}^{ion}]^a\tau)R_{air}$ / α, a constant at constant operating temperature.

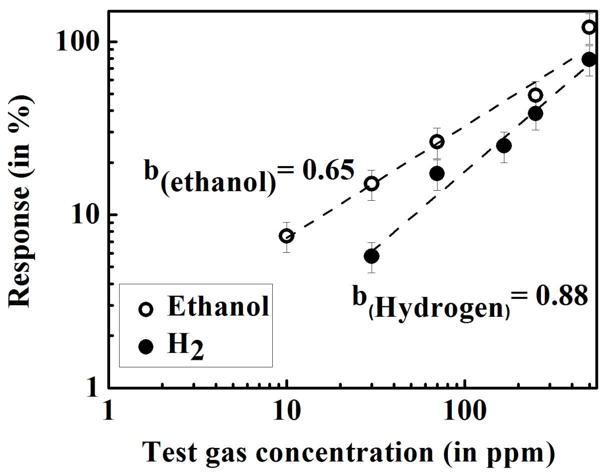

Fig. 6. Response vs. test gas concentration of 25 nm composite thin film at the operating temperature of 400 °C; gas flow rate: 100 cc/min.

TABLE VI
COMPARISON OF OUR EXPERIMENTAL DATA WITH AVAILABLE LITERATURE VALUES OF CuO BASED SENSING MATERIALS

Sensor material	Test gas (ppm)	τ_{res}	τ_{rec}	R_s (%)	O.T. (°C)	Ref.
CuO thin film	H_2 (10,000)	~10 min	~20 min	40	250	[2]
CuO nanostructures	H_2(100)	-	-	50	300	[42]
Porous CuO nanowires	H_2(60,000)	~2.5 min	~10 min	400	250	[14]
CuO/ZnO hetero contact	H_2(4000)	-	-	25	200	[1]
CuO–$CuFe_2O_4$ thin film	H_2(1250) H_2(2500)	190 s -	400 s -	40 79	295 295	[36]
CuO/ZnO hetero contacts	H_2(4000)	-	-	130	400	[15]
CuO–$CuFe_2O_4$ thin film	H_2(500)	58 s	221 s	79	400	our work
CuO nano rods	Ethanol (2000)	-	-	160	300	[3]
CuO nano wires	Ethanol (500)	-	-	24	300	[4]
CuO nano wires	Ethanol (1000)	110 s	120 s	50	240	[5]
CuO microspheres	Ethanol (200)	-	-	70	240	[6]
CuO thin film	Ethanol (12.5)	-	-	120	180	[7]
CuO–$CuFe_2O_4$ thin film	Ethanol (500)	90 s	450 s	130	450	our work

Figure 6 shows the variation of response of the 25 nm thin film sensor with gas concentration at the operating temperature of 400 °C. Gas sensing response is following the power law equation (eq. 22) for both the gases in the range of 10 ppm to 500 ppm. Response toward ethanol is slightly higher than that of hydrogen for similar concentration, i.e., this sensor is more sensitive toward ethanol than hydrogen. The obtained value of b is 0.65 for ethanol and 0.88 for hydrogen. This value of b toward ethanol is quite similar with the reported values, 0.677 and 0.54 for ZnO nano rods and nano structured sensing materials respectively [39], [40]. For hydrogen, the value of b was reported as 0.53 for ZnO thin films [41]. The value of b of these sensors was not as close to 0.5. Such deviation might occur due to the fact that the surface depletion or accumulation layer has some effect on the oxygen adsorption species at metal oxide surface when the grain diameter is close to double of that layer thickness ($2L_d$) [41]. At the operating temperature of 400 °C, both O^- and O^{2-} ion species formation are possible on metal oxide surface [38]; quantitative comparison of these ions at this operating temperature is not available in literature. So, the value of b power law exponent for hydrogen can be in the range of 0.5 to 1 at the operating temperature of 400 °C. The value 0.88 for hydrogen in our case gives an indication of higher concentration of O^- ion than O^{2-} on sensor surface at the operating temperature of 400 °C. Similarly, for ethanol the value can be in the range of 0.08 to 1 at the operating temperature of 400 °C, but the value 0.65 indicates the reduction of ethanol through the formation of acetaldehyde on the sensor surface.

The ethanol and H_2 sensing properties of various CuO nano structures in the literature are summarized in Table VI. Few of them reported higher response in comparison to the current work but at the cost of very high gas concentration [3], [14], [15]. And short response time was observed in this present study among the values reported recently in the literature of CuO sensors.

V. CONCLUSION

The self-organized CuO–$CuFe_2O_4$ thin films showed p-type semiconductor behaviour with increase in electrical resistance upon exposure to hydrogen or ethanol gas. Good fitting of response or recovery curve with single site gas adsorption model indicates that the reaction had occurred only on the surface of thin films. The developing process of this porous microstructure of top CuO layer is interesting as this kind of sensors have shown improved sensing properties toward reducing gases (e.g. ethanol and hydrogen) compared to the CuO thin film sensors fabricated by other techniques already reported. The best sensing performance was observed for the 25 nm thin film at an operating temperature of 400 °C with a response of 79% toward 500 ppm of H_2 and the response and recovery times obtained at this temperature are ~60 s and ~220 s, respectively. This 25 nm thin film sample also exhibited 128% response toward 500 ppm of ethanol with 90 seconds response time at the operating temperature of 400 °C. Also, we have demonstrated the variation of response of the sensors for a wide range of test-gas concentration. Due to these promising results, we believe that an optimised fabrication of this composite material could be a cheap potential gas sensing candidate only for local target oriented applications where the presence of other interfering gases is in negligible amount (e.g. in breathalyzer, water electrolysis plant). For example, the typical composition of exhaled air is 5.0–6.3% water vapour, 74.4% nitrogen, 13.6–16.0% oxygen, 4.0–5.3% carbon dioxide, <0.1% microbes or volatile organic compounds [43], [44]. Presence of humidity plays a significant role on sensing performance of metal oxide semiconductors at low operating temperatures (<250 °C) by the formation of HO^- at the surface of the semiconductor. Wang *et al.* [45] reported decrease in response of CuO

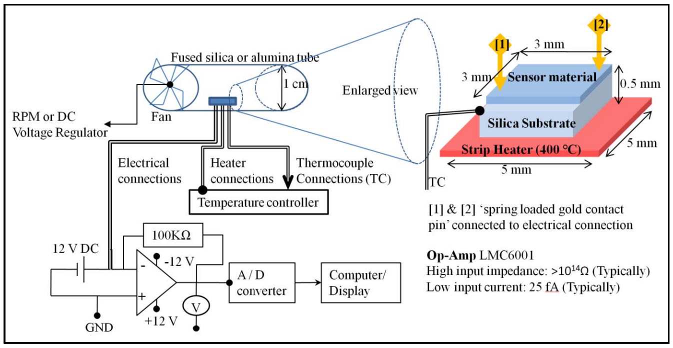

Fig. 7. A schematic illustration of the proposed sensing device using CuO-$CuFe_2O_4$ composite thin film.

sensor toward reducing gas (e.g. ethanol) with increase in relative humidity at the operating temperature of 220 °C. Morimoto *et al.* [46] showed that the most of the water content desorbed from metal oxides (e.g TiO_2, ZnO, α-Fe_2O_3) surface at the operating temperature of 400 °C. So, the effect of moisture on this sensor performance can be negligible as it will be operated at 450 °C. In our earlier studies, it was observed that the response of the same sample toward CO_2 was very slow with response time of ∼9.5 hour and maximum response of ∼50% was observed at 250 °C which reduced below 10% at higher operating temperature (400 °C) [47]. So, fabrication of a practical breath-alcohol tester can be possible for its fast response time (1.5 min) and recovery time (7.5 min) with high response toward ethanol at 450 °C. Similarly, it can be used as cheap alarm for hydrogen-leakage, e.g., at water electrolysis plant (where the presence of alcohol or volatile organic compound is negligible or rare). A schematic illustration of the proposed sensing device is given in the figure 7. This proposed sensor should be operated at normal air atmosphere (∼20% O_2), where oxygen will not vary to that much extent in this environment. Though, in our future work, we plan to investigate the effect of oxygen concentration at ambient atmosphere on the sensing performance of this CuO–$CuFe_2O_4$ composite sensing material.

Acknowledgment

The authors thank IRCC facility, IIT Bombay for the broadband dielectric spectrometer (BDS) facility.

References

[1] C. S. Dandeneau, Y.-H. Jeon, C. T. Shelton, T. K. Plant, D. P. Cann, and B. J. Gibbons, "Thin film chemical sensors based on *p*-CuO/*n*-ZnO heterocontacts," *Thin Solid Films*, vol. 517, no. 15, pp. 4448–4454, 2009, doi: 10.1016/j.tsf.2009.01.054.

[2] N. D. Hoa, S. Y. An, N. Q. Dung, N. Van Quy, and D. Kim, "Synthesis of p-type semiconducting cupric oxide thin films and their application to hydrogen detection," *Sens. Actuators B, Chem.*, vol. 146, no. 1, pp. 239–244, 2010, doi: 10.1016/j.snb.2010.02.045.

[3] C. Wang, X. Q. Fu, X. Y. Xue, Y. G. Wang, and T. H. Wang, "Surface accumulation conduction controlled sensing characteristic of p-type CuO nanorods induced by oxygen adsorption," *Nanotechnology*, vol. 18, no. 14, pp. 145506–145511, 2007, doi: 10.1088/0957-4484/18/14/145506.

[4] H. T. Hsueh *et al.*, "Ethanol gas sensor of crabwise CuO nanowires prepared on glass substrate," *J. Electrochem. Soc.*, vol. 158, no. 4, pp. J106–J109, 2011, doi: 10.1149/1.3551505.

[5] P. Raksa, A. Gardchareon, T. Chairuangsri, P. Mangkorntong, N. Mangkorntong, and S. Choopun, "Ethanol sensing properties of CuO nanowires prepared by an oxidation reaction," *Ceram. Int.*, vol. 35, no. 2, pp. 649–652, 2009, doi: 10.1016/j.ceramint.2008.01.028.

[6] G. Zhu, H. Xu, Y. Xiao, Y. Liu, A. Yuan, and X. Shen, "Facile fabrication and enhanced sensing properties of hierarchically porous CuO architectures," *ACS Appl. Mater. Interfaces*, vol. 4, no. 2, pp. 744–751, 2012, doi: 10.1021/am2013882.

[7] A. S. Zoolfakar *et al.*, "Nanostructured copper oxides as ethanol vapour sensors," *Sens. Actuators B, Chem.*, vol. 185, pp. 620–627, Aug. 2013, doi: 10.1016/j.snb.2013.05.042.

[8] L. Liao *et al.*, "Multifunctional CuO nanowire devices: p-type field effect transistors and CO gas sensors," *Nanotechnology*, vol. 20, no. 8, p. 085203, 2009, doi: 10.1088/0957-4484/20/8/085203.

[9] Y.-S. Kim, I.-S. Hwang, S.-J. Kim, C.-Y. Lee, and J.-H. Lee, "CuO nanowire gas sensors for air quality control in automotive cabin," *Sens. Actuators B, Chem.*, vol. 135, no. 1, pp. 298–303, 2008, doi: 10.1016/j.snb.2008.08.026.

[10] X. Zhou, Q. Cao, H. Huang, P. Yang, and Y. Hu, "Study on sensing mechanism of CuO–SnO_2 gas sensors," *Mater. Sci. Eng. B*, vol. 99, nos. 1–3, pp. 44–47, 2003, doi: 10.1016/S0921-5107(02)00501-9.

[11] J. Chen, K. Wang, L. Hartman, and W. Zhou, "H_2S detection by vertically aligned CuO nanowire array sensors," *J. Phys. Chem. C*, vol. 112, no. 41, pp. 16017–16021, 2008, doi: 10.1021/jp805919t.

[12] N. S. Ramgir *et al.*, "Sub-ppm H_2S sensing at room temperature using CuO thin films," *Sens. Actuators B, Chem.*, vol. 151, no. 1, pp. 90–96, 2010, doi: 10.1016/j.snb.2010.09.043.

[13] Q. Zhang *et al.*, "CuO nanostructures: Synthesis, characterization, growth mechanisms, fundamental properties, and applications," *Prog. Mater. Sci.*, vol. 60, pp. 208–337, Mar. 2014, doi: 10.1016/j.pmatsci.2013.09.003.

[14] N. D. Hoa, N. Van Quy, H. Jung, D. Kim, H. Kim, and S.-K. Hong, "Synthesis of porous CuO nanowires and its application to hydrogen detection," *Sens. Actuators B, Chem.*, vol. 146, no. 1, pp. 266–272, 2010, doi: 10.1016/j.snb.2010.02.058.

[15] S. Aygün and D. Cann, "Hydrogen sensitivity of doped CuO/ZnO heterocontact sensors," *Sens. Actuators B, Chem.*, vol. 106, no. 2, pp. 837–842, 2005, doi: 10.1016/j.snb.2004.10.004.

[16] O. Lupan *et al.*, "Influence of CuO nanostructures morphology on hydrogen gas sensing performances," *Microelectron. Eng.*, vol. 164, pp. 63–70, Oct. 2016, doi: 10.1016/j.mee.2016.07.008.

[17] P. Samarasekara, N. T. R. N. Kumara, and N. U. S. Yapa, "Sputtered copper oxide (CuO) thin films for gas sensor devices," *J. Phys., Condens. Matter*, vol. 18, no. 8, pp. 2417–2420, 2006, doi: 10.1088/0953-8984/18/8/007.

[18] C. V. G. Reddy, S. V. Manorama, and V. J. Rao, "Preparation and characterization of ferrites as gas sensor materials," *J. Mater. Sci. Lett.*, vol. 19, no. 9, pp. 775–778, 2000, doi: 10.1023/A:.1006716721984.

[19] S. Singh, B. C. Yadav, R. Prakash, B. Bajaj, and J. R. Lee, "Synthesis of nanorods and mixed shaped copper ferrite and their applications as liquefied petroleum gas sensor," *Appl. Surf. Sci.*, vol. 257, no. 24, pp. 10763–10770, 2011, doi: 10.1016/j.apsusc.2011.07.094.

[20] S. Tao, F. Gao, X. Liu, and O. T. Sørensen, "Preparation and gas-sensing properties of $CuFe_2O_4$ at reduced temperature," *Mater. Sci. Eng. B*, vol. 77, no. 2, pp. 172–176, 2000, doi: 10.1016/S0921-5107(00)00473-6.

[21] T. P. Sumangala, C. Mahender, A. Barnabe, N. Venkataramani, and S. Prasad, "Structural, magnetic and gas sensing properties of nanosized copper ferrite powder synthesized by sol gel combustion technique," *J. Magn. Magn. Mater.*, vol. 418, pp. 48–53, Nov. 2016, doi: 10.1016/j.jmmm.2016.02.053.

[22] T. P. Sumangala *et al.*, "Study on the effect of cuprite content on the electrical and CO_2 sensing properties of cuprite-copper ferrite nanopowder composites," *J. Alloys Compounds*, vol. 695, pp. 937–943, Feb. 2017, doi: 10.1016/j.jallcom.2016.10.197.

[23] T. Ishihara, K. Kometani, M. Hasida, and Y. Takita, "Application of mixed oxide capacitor to the selective carbon dioxide sensor: I. Measurement of carbon dioxide sensing characteristics," *J. Electrochem. Soc.*, vol. 138, no. 1, pp. 173–176, 1991, doi: 10.1149/1.2085530.

[24] Y. F. Gu, H. M. Ji, B. Zhang, and T. X. Xu, "Preparation and CO_2 gas sensitive properties of CuO-$SrTiO_3$-based semiconductor thin films," *Key Eng. Mater.*, vols. 280–283, pp. 311–314, Feb. 2007, doi: 10.4028/www.scientific.net/KEM.280-283.311.

[25] J. C. Xu, G. W. Hunter, D. Lukco, C.-C. Liu, and B. J. Ward, "Novel carbon dioxide microsensor based on tin oxide nanomaterial doped with copper oxide," *IEEE Sensors J.*, vol. 9, no. 3, pp. 235–236, Mar. 2009, doi: 10.1109/JSEN.2008.2011953.

[26] G. Zhang and M. Liu, "Effect of particle size and dopant on properties of SnO_2-based gas sensors," *Sens. Actuators B, Chem.*, vol. 69, nos. 1–2, pp. 144–152, 2000, doi: 10.1016/S0925-4005(00)00528-1.

[27] A. Chapelle *et al.*, "Improved semiconducting $CuO/CuFe_2O_4$ nanostructured thin films for CO_2 gas sensing," *Sens. Actuators B, Chem.*, vol. 204, pp. 407–413, Dec. 2014, doi: 10.1016/j.snb.2014.07.088.

[28] A. Barnabé, A. Chapelle, L. Presmanes, and P. Tailhades, "Copper and iron based thin film nanocomposites prepared by radio frequency sputtering. Part I: Elaboration and characterization of metal/oxide thin film nanocomposites using controlled *in situ* reduction process," *J. Mater. Sci.*, vol. 48, no. 9, pp. 3386–3394, 2013, doi: 10.1007/s10853-012-7123-6.

[29] A. Chapelle, A. Barnabé, L. Presmanes, and P. Tailhades, "Copper and iron based thin film nanocomposites prepared by radio-frequency sputtering. Part II: Elaboration and characterization of oxide/oxide thin film nanocomposites using controlled *ex-situ* oxidation process," *J. Mater. Sci.*, vol. 48, no. 8, pp. 3304–3314, 2013, doi: 10.1007/s10853-012-7116-5.

[30] M.-H. Seo, M. Yuasa, T. Kida, J.-S. Huh, K. Shimanoe, and N. Yamazoe, "Gas sensing characteristics and porosity control of nanostructured films composed of TiO_2 nanotubes," *Sens. Actuators B, Chem.*, vol. 137, no. 2, pp. 513–520, 2009, doi: 10.1016/j.snb.2009.01.057.

[31] B.-J. Ahn, B. J. McCOY, and J. M. Smith, "Separation of adsorption and surface reaction rates: Dynamic studies in a catalytic slurry reactor," *AIChE J.*, vol. 31, no. 4, pp. 541–550, 1985, doi: 10.1002/aic.690310403.

[32] L. A. Arrua, B. J. McCoy, and J. M. Smith, "Effect of catalyst poisoning on adsorption and surface reaction rates in liquid-phase hydrogenation," *Ind. Eng. Chem. Res.*, vol. 29, no. 6, pp. 1050–1057, 1990, doi: 10.1021/ie00102a015.

[33] K. Mukherjee and S. B. Majumder, "Analyses of response and recovery kinetics of zinc ferrite as hydrogen gas sensor," *J. Appl. Phys.*, vol. 106, no. 6, p. 064912, 2009, doi: 10.1063/1.3225996.

[34] S. Ahlers, G. Müller, and T. Doll, "A rate equation approach to the gas sensitivity of thin film metal oxide materials," *Sens. Actuators B, Chem.*, vol. 107, no. 2, pp. 587–599, 2005, doi: 10.1016/j.snb.2004.11.020.

[35] S. K. Biswas and P. Pramanik, "Studies on the gas sensing behaviour of nanosized $CuNb_2O_6$ towards ammonia, hydrogen and liquefied petroleum gas," *Sens. Actuators B, Chem.*, vol. 133, no. 2, pp. 449–455, 2008, doi: 10.1016/j.snb.2008.03.004.

[36] A. Chapelle *et al.*, "Structural and gas-sensing properties of $CuO–Cu_xFe_{3-x}O_4$ nanostructured thin films," *Sens. Actuators B, Chem.*, vol. 153, no. 1, pp. 117–124, 2011, doi: 10.1016/j.snb.2010.10.018.

[37] M. Tonezzer, D. T. T. Le, T. Q. Huy, and S. Iannotta, "Dual-selective hydrogen and ethanol sensor for steam reforming systems," *Sens. Actuators B, Chem.*, vol. 236, pp. 1011–1019, Nov. 2016, doi: 10.1016/j.snb.2016.04.150.

[38] N. Barsan, M. Schweizer-Berberich, and W. Göpel, "Fundamental and practical aspects in the design of nanoscaled SnO_2 gas sensors: A status report," *Fresenius' J. Anal. Chem.*, vol. 365, no. 4, pp. 287–304, 1999, doi: 10.1007/s002160051490.

[39] Y. Chen, C. L. Zhu, and G. Xiao, "Reduced-temperature ethanol sensing characteristics of flower-like ZnO nanorods synthesized by a sonochemical method," *Nanotechnology*, vol. 17, no. 18, pp. 4537–4541, 2006, doi: 10.1088/0957-4484/17/18/002.

[40] E. Wongrat, P. Pimpang, and S. Choopun, "Comparative study of ethanol sensor based on gold nanoparticles: ZnO nanostructure and gold: ZnO nanostructure," *Appl. Surf. Sci.*, vol. 256, no. 4, pp. 968–971, 2009, doi: 10.1016/j.apsusc.2009.02.046.

[41] L. Rajan, P. Chinnamuthan, V. Krishnasamy, and V. Sahula, "An investigation on electrical and hydrogen sensing characteristics of RF sputtered ZnO thin-film with palladium Schottky contacts," *IEEE Sensors J.*, vol. 17, no. 1, pp. 14–21, Jan. 2017, doi: 10.1109/JSEN.2016.2620185.

[42] A. Umar, J.-H. Lee, R. Kumar, O. Al-Dossary, A. A. Ibrahim, and S. Baskoutas, "Development of highly sensitive and selective ethanol sensor based on lance-shaped CuO nanostructures," *Mater. Des.*, vol. 105, pp. 16–24, Sep. 2016, doi: 10.1016/j.matdes.2016.05.006.

[43] A. Guyton and J. Hall, "Physical principles of gas exchange; diffusion of oxygen and carbon dioxide through the respiratory membrane," in *Textbook of Medical Physiology*, 11th ed. Philadelphia, PA, USA: Saunders, 2005, ch. 39.

[44] J. D. Fenske and S. E. Paulson, "Human breath emissions of VOCs," *J. Air Waste Manage. Assoc.*, vol. 49, p. 5, pp. 594–598, 1999, doi: 10.1080/10473289.1999.10463831.

[45] F. Wang *et al.*, "A highly sensitive gas sensor based on CuO nanoparticles synthetized via a sol–gel method," *RSC Adv.*, vol. 6, no. 83, p. 79343, 2016, doi: 10.1039/c6ra13876d.

[46] T. Morimoto, M. Nagao, and F. Tokud, "Desorbability of chemisorbed water on metal oxide surfaces. I. Desorption temperature of chemisorbed water on hematite, rutile and zinc oxide," *Bull. Chem. Soc. Jpn.*, vol. 41, no. 7, pp. 1533–1537, 1968, doi: 10.1246/bcsj.41.1533.

[47] A. Chapelle, F. Oudrhiri-Hassani, L. Presmanes, A. Barnabé, P. Tailhades, "CO_2 sensing properties of semiconducting copper oxide and spinel ferrite nanocomposite thin film," *Appl. Surf. Sci.*, vol. 256, pp. 4715–4719, May 2010, doi: 10.1016/j.apsusc.2010.02.079.

Saptarshi De received the B.Sc. (Hons.) degree in physics from Calcutta University, Kolkata, India, in 2008, and the M.Sc. degree in physics with a specialization in molecular spectroscopy from Banaras Hindu University, Varanasi, India, in 2010. He is currently pursuing the Ph.D. degree with the Department of Metallurgical Engineering and Materials Science, Indian Institute of Technology Bombay, India. His research interests include solid-state chemical sensors, *in situ* spectroscopic study, and sensing mechanism.

Narayanan Venkataramani (SM'16) received the Ph.D. degree in materials science from the Indian Institute of Technology Bombay, India, in 1986. He is currently a Professor and the Head of the Department of Metallurgical Engineering and Materials Science, Indian Institute of Technology Bombay. His current research interests include the synthesis and characterization of polycrystalline, single crystal and thin-film oxide materials; structure property correlation work in the areas of bulk polycrystalline, nanocrystalline thin-film and thick-films of ferrites, and magnetoelectric composites. He is a Life Member of the Materials Research Society of India.

Shiva Prasad received the M.Sc. degree in physics from IIT Delhi in 1973 and the Ph.D. degree from the University of Delhi in 1978. After Post-Doctoral Research at the Laboratory of Magnetism, CNRS, Bellevue, France, and the California Institute of Technology, Pasadena, CA, USA, he joined the Indian Institute of Technology Bombay, India, as a Faculty Member in 1980. He recently retired as Professor of Physics, Indian Institute of Technology Bombay, and has joined as the Director-General of the Institute of Infrastructure Technology Research and Management, Ahmedabad, India. He was awarded "Officier des Palmes Academiques" in 2007 and "Chevalier de la Legion d'Honneur" in 2011 by the French Government. His research interests include magnetic properties of nano-crystalline thin-films of oxide materials.

Rajiv Onkar Dusane received the Ph.D. degree in physics from the University of Poona, India, in 1989. He is currently a Professor with the Department of Metallurgical Engineering and Materials Science, Indian Institute of Technology Bombay, India. His current research interests include plasma processing, surface nano-engineering; synthesis and characterization of amorphous and nanocrystalline thin-films of elemental semiconductors and alloys, silicon nano devices, for applications such as thin-film solar cells, thin-film transistors for flat panel displays, MEMS devices, and nuclear detections.

Lionel Presmanes received the Ph.D. degree for his thesis work on ferrite thin films for magneto-optical storage. Since 1997, he has been with the CIRIMAT Laboratory, University Paul Sabatier, Toulouse, and is also CNRS Researcher since 2001. His research interests are focused on the preparation of sputtered oxide and nano-composites thin films and the study of their microstructure as well as their electrical, magnetic, and optical properties. He developed sputtered ferrite thin films to be integrated as sensitive layers in magneto-optical disks and micro-bolometers (IR sensors). His work is currently focused on transparent conducting oxides and semiconductor sensitive layers for gas sensors.

Yohann Thimont received the Ph.D. degree in chemistry of materials from the University de Caen Basse-Normandie, France, in 2009, for $YBa_2Cu_3O_7$ thin-films depositions and characterization. He held a nine month post-doctoral position based on the study and the deposition of TCO thin films at the LRCS Laboratory, Amiens, France. He then returned to Caen as a Temporary Teacher and a Researcher in superconductor thematic for two years then held another post-doctoral position at Caen for one year which was devoted to the synthesis and characterization of thermoelectric silicides. He has been an Assistant Professor with the CIRIMAT Laboratory, Toulouse, France, since 2013. His research interests include the thin films synthesis and topographic, electrical, magnetic, and optical characterizations.

Philippe Tailhades received the Ph.D. degree in material science in 1988 and the Habilitation à Diriger les Recherches in 1994. He is currently the Vice Director of the Centre Interuniversitaire de Recherche et d'Ingénierie des Matériaux, Toulouse, France. His research interests include the preparation of original metallic oxides, especially spinel ferrites, in the form of fine powders, thin films, or bulk ceramics and the study of their magnetic, electric, and optical properties. He also works on the preparation of special metallic powders and on laser additive manufacturing. He received the Silver Medal of CNRS, France, in 2000.

Valérie Baco-Carles received the Ph.D. degree in material science from Paul Sabatier University, France, in 1995. She is currently a CNRS Research Engineer with the Centre Interuniversitaire de Recherche et d'Ingénierie des Matériaux (CIRIMAT), Toulouse, France. Her research interests include the preparation of mixed metallic oxalates, oxides powders and micro- or nano-metallic powders. She also works on the synthesis of ceramics and cermets. She studies the mechanical, magnetic, electrical, or brazing properties of these materials. She is involved in several technology transfer operations. Notably, spongy metallic iron powder used as heating elements in thermal batteries (aeronautical and spatial applications) was industrially produced using a co-patent of CIRIMAT.

Corine Bonningue received the Ph.D. degree in chemistry from the Paul Sabatier University de Toulouse, France, in 1980. She is currently an Assistant Professor with the CIRIMAT Laboratory, Chemistry Department, Paul Sabatier University, France. Her current research interests include functional metal oxide powders, ceramics, and thin films (prepared by PVD technique).

Sumangala Thondiyanoor Pisharam received the B.Sc. and M.Sc. degrees in physics from the University of Calicut, Kerala, India, and the Ph.D. degree from the Department of Metallurgical Engineering and Materials Science, Indian Institute of Technology Bombay in 2015. Her research interest is in metal oxide semiconductors mainly ferrites. Her work is on the synthesis of ferrites in the form of nano powders, their casting to thick film and the study of their structural, micro structural, magnetic, electric, and gas sensing properties. She received the Charpark Fellowship from the French Embassy, India, in 2012.

Antoine Barnabé received the Ph.D. degree in chemistry of materials from the University de Caen-Basse Normandie, France, in 1999. He held a post-doctoral position at Northwestern University, Evanston, IL, USA, in 2000. He is currently a Professor with the CIRIMAT Laboratory, Paul Sabatier University, France. His current research interests are mainly focused on functional metal oxide powders, ceramics and thin films prepared by PVD technique from the preparation to the advanced structural, microstructural, and chemical characterizations. He is responsible for the Microcharacterization Center R. CASTAING, Toulouse.